Biocompatible Pillararene-Assembly-Based Carriers for Dual Bioimaging

Huacheng Zhang,[†] Xing Ma,[‡] Kim Truc Nguyen,[†] and Yanli Zhao[†,‡,*]

[†]Division of Chemistry and Biological Chemistry, School of Physical and Mathematical Sciences, Nanyang Technological University, 21 Nanyang Link, 637371 Singapore and [‡]School of Materials Science and Engineering, Nanyang Technological University, 50 Nanyang Avenue, 639798, Singapore

ABSTRACT Present research provides a successful example to use biocompatible pillararene-based assemblies for delivering mixed dyes in dual bioimaging. A series of tadpole-like and bola amphiphilic pillararenes 1–4 were synthesized by selectively employing water-soluble ethylene glycols and hydrophobic alkyl units as the starting materials. In comparison with their monomers, these amphiphilic pillararenes not only show improved biocompatibility to cells but also could form homogeneous supramolecular self-assemblies. Interestingly, different types of amphiphilic pillararene-based assemblies exhibit various performances on the delivery of dyes with different aqueous solubility. All assemblies can deliver water-soluble rhodamine B to cells, while only tadpole-like amphiphilic pillararene-based assemblies performed better on delivering hydrophobic fluorescein isothiocyanate for imaging. In addition, pillararene derivatives 1, 3, and 4 could complex with a viologen guest, further forming stable assemblies for bioimaging. In such cases, the assembly formed from the complex of tadpole-like amphiphile pillararene 1 with the viologen guest performed better in delivering mixed dyes. Finally, an anticancer drug, doxorubicin, was successfully delivered to cells by using the pillararene-based assemblies. The current research has determined the capacities of pillararene-based assemblies to deliver different dyes for bioimaging and paves the way for using these biocompatible carriers toward combined cancer therapy.

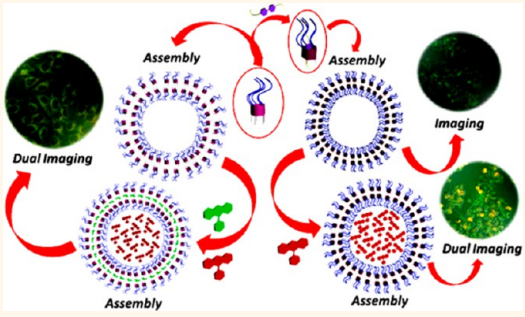

KEYWORDS: cytotoxicity · dual bioimaging · host–guest interaction · pillararenes · self-assembly

Self-assemblies constructed by pillararenes[1–6] have attracted much attention of chemists over the past 5 years. Various topological morphologies[7–9] of pillararene-based supramolecular assemblies[10,11] along with fundamental principles for assembling[12–14] have been developed so far. For example, UV/vis-responsive zero-dimensional (0D) supramolecular architectures were prepared by using azobenzene covalently modified pillar[5]arenes,[15] showing a morphology shift between hollow and solid spheres upon alternate exposure to visible and UV light. Similarly, spherical assemblies prepared by fluorescein isothiocyanate (FITC)-modified pillar[5]arenes[16] exhibited thermoresponsive properties by changing the external temperature. In these two cases,[15,16] owing to poor host–guest interactions[1–3] between the pillar[5]arene cavity and functional units with unmatched sizes, the functional groups were excluded from the pillararene cavity in organic solvents. Layered spherical structures were subsequently formed through solvophobic effects and supramolecular interactions between these functional groups.[15,16] Thus, a question was raised—what will happen by coupling the guest molecules with the pillararenes? We then added a linear molecule with two viologen units into acetone solution of 1,4-dimethoxypillar[5]arene (DMpillar).[17] In contrast to no regular aggregates being observed in acetone solution of individual DMpillar, the inclusion complex between the biviologen guest and DMpillar formed spherical 0D supramolecular architectures, indicating that the introduction of suitable guests can influence the morphologies of pillararene-based assemblies. Furthermore, we covalently modified pillararenes with viologen units[18] and found that, by gradually increasing concentrations, viologen-modified pillararenes formed self-inclusion, supramolecular daisy chains and linear polymeric assemblies one by one. The driving force in this assembly process was definitely the host–guest interactions.[18] Very recently, by employing the dendritic pillararene host, dynamic supramolecular assemblies prepared through the host–guest interactions between a pillararene trimer and a biviologen

* Address correspondence to zhaoyanli@ntu.edu.sg.

Received for review June 3, 2013 and accepted August 3, 2013.

Published online August 03, 2013
10.1021/nn402777x

© 2013 American Chemical Society

guest presented multidimensional morphology changes.[17] The dynamic supramolecular assemblies can be transformed along vesicular structures (0D), linear objects (one-dimensional, 1D), layers (two-dimensional, 2D), and stacked layers (three-dimensional, 3D) upon increasing the concentrations, providing a novel strategy for the morphology control. Fabricating these assemblies is a kind of building-block game with the controlling strategies, such as supramolecular interactions and solvophobic effects, as well as proper external stimulus methods.[19] In addition, all the assemblies obtained expand the horizon for fabricating pillararene-based topological supramolecular materials and provide theoretical foundations for further applications, for example, in biomimetics and biomedicine.[20−22]

In comparison with other hosts, such as cyclodextrins[23] and calixarenes,[24] studies on applying pillararenes and their assemblies to biomedicine are still limited. Up to now, only two papers reported the toxicity[25] and biomimicking[26] of aqueous soluble pillararenes. On one hand, current research regarding the pillararene assemblies is still on the stage of morphology studies. On the other hand, poor aqueous solubility of pillararenes[1−3] is deemed as the key problem and limits their biomedical applications, leading to high toxicity to biological systems.[27−29] For instance, both DMpillar[5] and DBpillar[6] (1,4-dibutoxypillar[5]arene, Scheme 1) have very poor aqueous solubility, although they can be dissolved in dimethyl sulfoxide (DMSO). The DMSO solution of DMpillar or DBpillar was cytotoxic and harmful (Figure S1 in the Supporting Information (SI)). We found that DMSO solvent itself has high toxicity to HeLa cells, determined by the MTT ((3-(4,5-dimethylthiazol-2-yl)-2,5-diphenyltetrazolium bromide) assay,[30−33] and the toxicity was decreased a lot upon increasing the volume ratio of H_2O in the mixed DMSO/H_2O solvent (Figure S1a in the SI). If aqueous solubility of pillararene derivatives is improved, by dissolving them in much lower amount of DMSO-containing DMSO/H_2O solvent, the toxicity should be significantly decreased. To confirm this hypothesis, dihydroxypillar[5]arene[6] (DHpillar) was prepared after the demethylation reaction of DMpillar (Scheme 1). DHpillar can be dissolved in mixed DMSO/H_2O solvent with low volume ratio (10%) of DMSO. The MTT assay of DHpillar in the mixed solvent was subsequently performed, indicating that the cytotoxicity of the DHpillar solution was reduced in comparison with those of DMpillar and DBpillar (Figure S1b−d in the SI). Encouraged by these results, if we introduce more biocompatible functional groups with good aqueous solubility onto pillararenes, obtained pillararene derivatives may expand their application prospects into the area of biomedicine.[27−29]

Herein, a series of amphiphilic pillararene derivatives (**1**−**4**, Scheme 1) was synthesized by selectively introducing water-soluble ethylene glycol groups and hydrophobic alkyl groups onto pillararenes. In comparison with their monomers, the derivatives not only show improved biocompatibility but also form homogeneous supramolecular self-assemblies above critical assembly concentration (CAC), exhibiting good performance on the delivery of mixed dyes to cells for dual bioimaging. Exploring potential applications of pillararenes in biomedicine is important for providing more carrier candidates for bioimaging and drug delivery. One major purpose of delivering fluorescent dyes into cells is to distinguish organelles within cells for tracking and diagnostics applications. However, the main disadvantage of using fluorescent dyes in the cell imaging is their low cell internalization efficiency. Thus, the dye carriers are needed to improve the imaging efficiency of dyes. To fully utilize the advantages of pillararene-based assemblies, several dyes were employed in our work, including rhodamine B (RhB), FITC, and viologen. We would like to provide a proof-of-concept by using these dye models in order to examine the capability of the pillararene-based assemblies for bioimaging and drug delivery. In the research, the mechanisms of the self-assembly as well as the influence of structures with different length of hydrophobic units on cytotoxicity and bioimaging were investigated. Furthermore, the feasibility of delivering a real anticancer drug, doxorubicin (Dox), by using these pillararene-based assemblies was confirmed *in vitro*.

RESULTS AND DISCUSSION

Design and Synthesis of Novel Pillararenes. To improve aqueous solubility and reduce cytotoxicity of pillararenes, water-soluble and biodegradable ethylene glycols[28] were employed to functionalize pillararenes through click reaction[15−18] with high synthetic efficiency. Alkynyl pillararene derivatives **5**−**7** were synthesized first by mixing corresponding alkynyl dihydroxybenzene derivatives with paraformaldehyde and boron trifluoride diethyl etherate in refluxing 1,2-dichloroethane under nitrogen atmosphere (Scheme 1).[1−3] It should be noted that, according to previous literature reports,[34,35] asymmetric synthesis of pillararenes can result in diverse conformers, such as partial cone, 1,2-alternate, 1,3-alternate, and cone. After being purified by flash column chromatography with CH_2Cl_2/*n*-hexane (v/v = 2:3−9:1) as gradient eluent, pure alkynyl pillararenes **5** and **6** with C_5 symmetric structures were obtained and confirmed based on their relatively simple ^1H and ^{13}C NMR spectra shown in the SI.[35] The obtained pure alkynyl pillararenes **5**−**7** further reacted with azido ethylene glycols through the copper(I)-catalyzed Huisgen-type azide−alkyne cycloaddition[15−18] in refluxing acetone under nitrogen atmosphere, affording crude products (Scheme S1 in the SI). Finally, compounds **1**−**4** were obtained in high yields over 80% after the purifications by flash column chromatography with MeOH/CH_2Cl_2 (v/v = 1:19−1:9) as gradient eluent and were fully characterized by NMR, mass spectrometric, and elemental analysis (see Materials and Methods section and the SI).

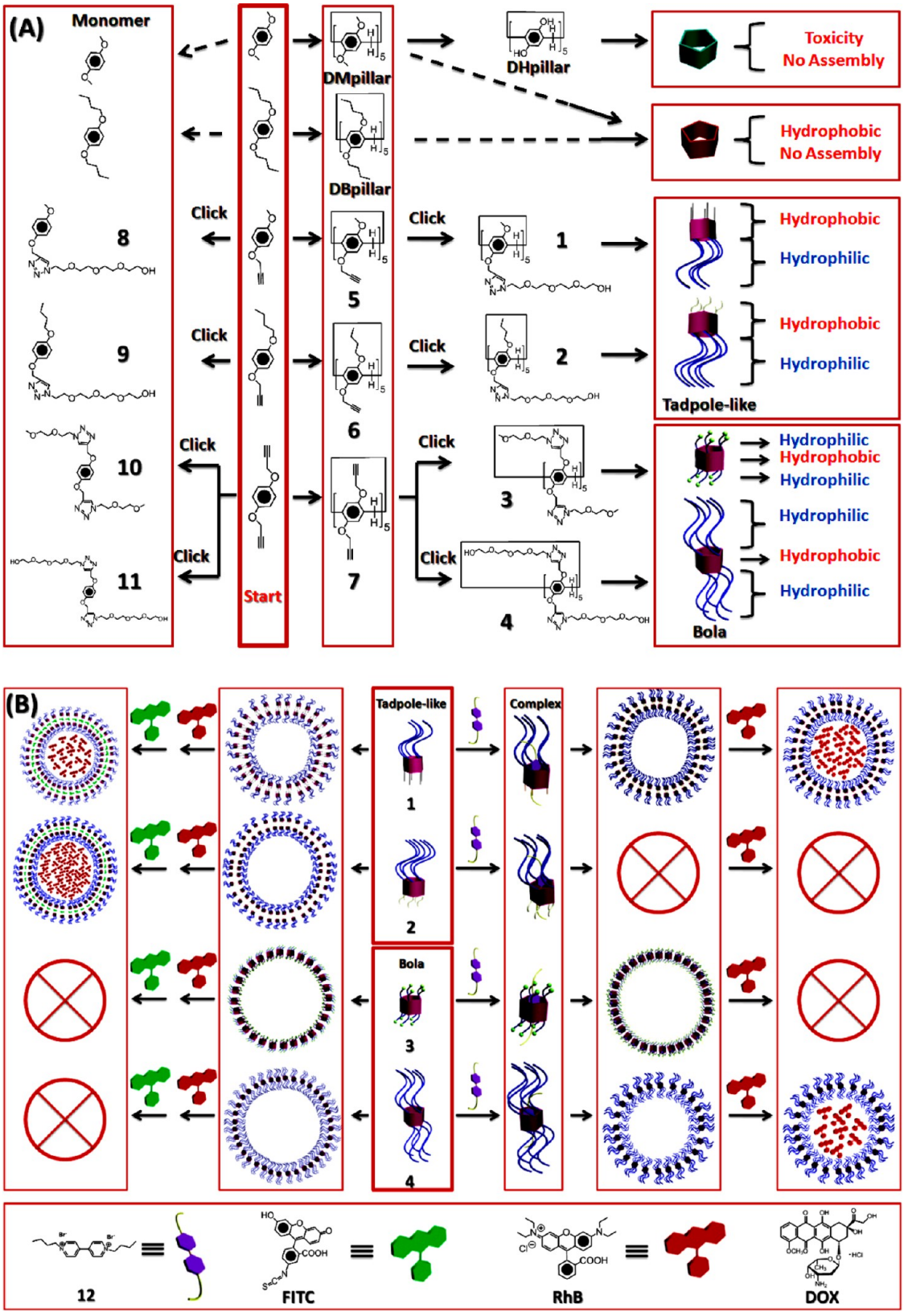

Scheme 1. (A) Synthesis and structural representations of DMpillar, DHpillar, DBpillar, and compounds 1−11. (B) Illustrative mechanism for dual bioimaging by using biocompatible pillararene-based assemblies to deliver 12, FITC, and RhB.

As compared to DMpillar and DBpillar, the solubility of compounds **1**−**4** in H_2O is significantly improved on account of introducing ethylene glycol groups and triazole rings to the pillararene structures.[28] Compound **4** dissolves well in H_2O (1 mM), forming an opalescent solution. Having extra hydrophobic alkyl chains on

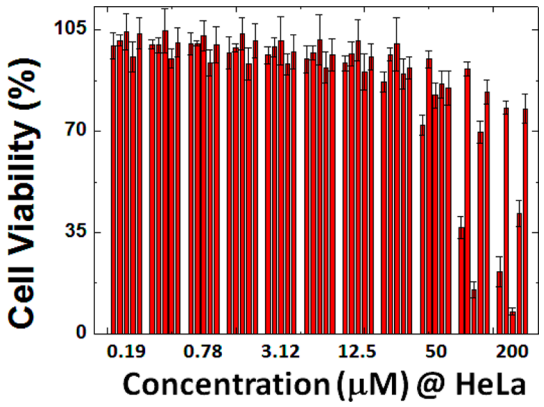

Figure 1. Viability of HeLa cells after being treated with DHpillar and compounds 1−3 in DMSO/H_2O (v/v = 1: 9) solvent and compound 4 in H_2O for 24 h. Five columns in each group from left to right under the same concentration indicate the cell viabilities after treatment with DHpillar and compounds 1−4.

pillararenes, compounds **1**−**3** have to be dissolved in aqueous solution (1 mM) containing a small amount of DMSO (10% volume ratio).

As expected, the improved aqueous solubility lowered the cytotoxicity of obtained pillararenes. A small amount of DMSO used in the mixture solvent has low cytotoxicity with little effect on the MTT assay (Figure S1a in the SI). In comparison with DHpillar, the biocompatibility of compounds **1**−**4** was remarkably improved with the concentrations below 50 μM according to the MTT assay, leading to the increase of the cell viability (Figure 1). Above the concentration of 100 μM, however, compound **2** is more toxic to cells than DHpillar, probably caused by possessing long hydrophobic alkyl chains.[27−29]

Characterization of Pillararene-Based Assemblies. To characterize the micromorphology and diameters of the assemblies formed by the amphiphilic pillararenes **1**−**4** in solution, transmission electron microscopy (TEM) and dynamic light scattering (DLS) were employed. As shown in Figure 2, spherical vesicular structures with diameters of around 80−500 nm were observed in these solutions (0.04 mM) by negative-stained TEM. These spherical assemblies could be sustained in solutions at 300 K for about 1 week. The sizes and size distributions of these nanospheres determined by TEM were further confirmed by DLS (Figure 2). Since DLS determines swollen samples (Figures S2−S5 in the SI), it is reasonable that the measured mean diameters (40−300 nm) by DLS have little variations from those observed by microscopic methods (Tables S1−S4 in the SI).[15−18]

Furthermore, the CAC of these amphiphilic pillararenes **1**−**4** was determined to be around 0.01−0.02 mM by DLS in a variable concentration scale (Figures S2−S5 and Tables S1−S4 in the SI). It is understandable that hydrophobic effect is the driving force in the formation of these vesicular assemblies by amphiphilic pillararenes in solution.[36−38] According to a geometric packing model,[15−18,36−38] owing to their cylindrical-like shapes, tadpole-like compounds **1** and **2** are assumed to self-assemble into ordered bilayer membranes above CAC with alkyl units located inside the bilayers and ethylene glycol units facing the inner and outer aqueous solution (Scheme 1B). Since compounds **3** and **4** are bola-like amphiphiles[36−38] with two hydrophilic ethylene glycol units at both ends, they aggregate orderly above CAC into lamellar structures with water molecules inside the cores (Scheme 1B).

In a control study, four monomers **8**−**11** of these amphiphilic pillararenes were synthesized by using the copper(I)-catalyzed Huisgen-type azide−alkyne cycloaddition with corresponding alkynyl dihydroxybenzene derivatives as the starting materials (see Materials and Methods section).[15−18] It was found that all four monomers have similar aqueous solubility with related amphiphilic pillararenes. In addition, monomers **8**, **10**, and **11** have similar low cytotoxicity with compounds **1**, **3**, and **4**, respectively. However, monomer **9** is more toxic than its pillar[5]arene analogue, **2**, and other monomers at the same concentration measured (Figure S6 in the SI). TEM was employed to examine the possible aggregates of these monomers under the same preparation conditions. However, no regular aggregates were formed in these samples, and only some occasionally formed irregular shapes were observed by TEM (Figure S7 in the SI). In comparison with their monomers **8**−**11**, amphiphilic pillararenes **1**−**4** with relatively low cytotoxicity have better capacity to form regular vesicular self-assemblies on account of their unique cylindrical-like structures.

Characterization of Inclusion Complexes between Pillararenes and Guests. Viologen, a fluorescent dye and the most suitable guest for pillararenes,[1−3] was chosen to be delivered by using the pillararene-based assemblies. Although viologen is toxic, it still can be used as a dye model in the delivery systems.[25] Here, we would like to provide a proof-of-concept by using this dye model in order to examine the capability of the pillararene-based assemblies for bioimaging. Thus, a viologen derivative, water-soluble compound **12** was synthesized through a simple substitution reaction in high yield (see the SI for experimental details)[15−18] and was used as a model dye for delivery. Owing to size effects and forming donor−acceptor pairs,[1−3] viologen can be easily included by the cavity of pillar[5]arenes in a 1:1 molar ratio. Compared to aqueous solutions containing individual **1**−**4** and **12**, after adding **12** into the solutions of compounds **1**−**4**, clear color change from colorless to yellow brown induced by the charge transfer between pillararenes and viologen was observed, indicating that the host−guest inclusion complexes were formed.[15−18] The complexation between amphiphilic pillararenes **1**−**4** and **12** was further confirmed by ^{1}H NOESY NMR spectroscopy, showing strong correlations

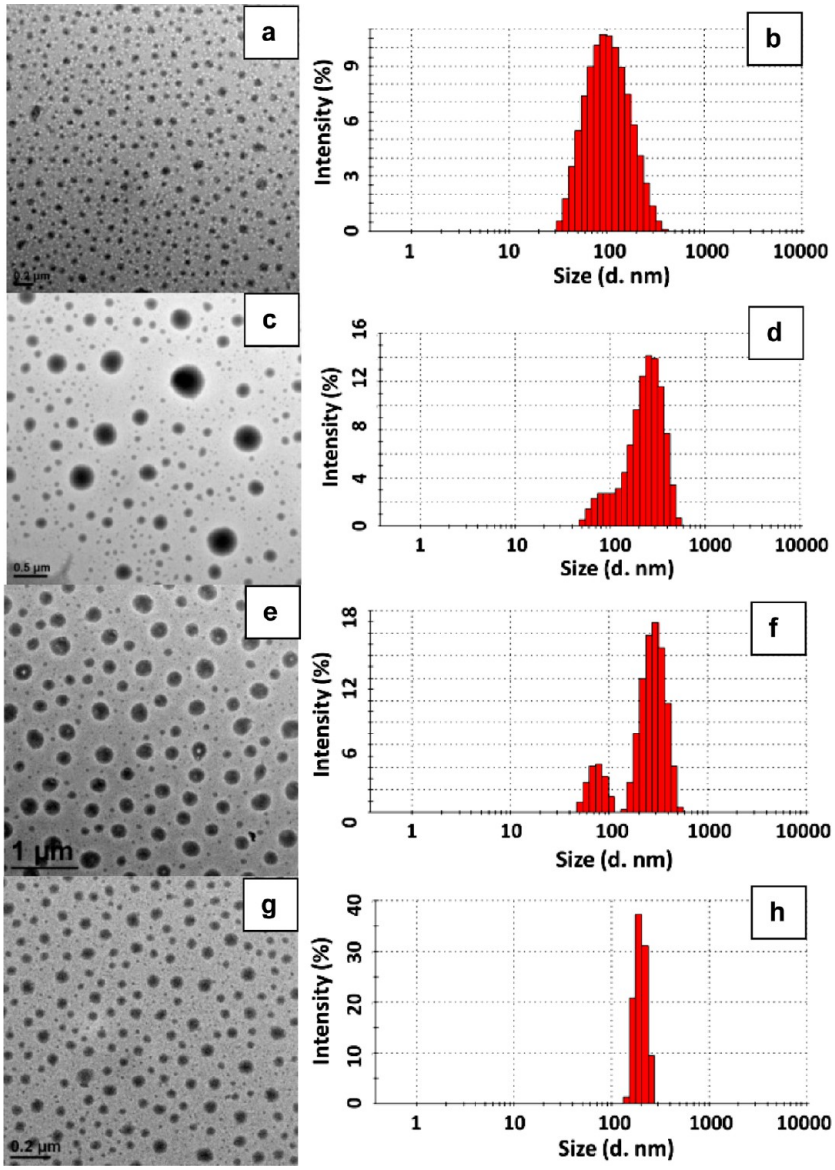

Figure 2. Micromorphology of compound 1 (a, 0.040 mM, scale bar = 0.2 μm), 2 (c, 0.040 mM, scale bar = 0.5 μm), and 3 (e, 0.040 mM, scale bar = 1.0 μm) in DMSO/H_2O (v/v = 1:9), as well as 4 (g, 0.040 mM, scale bar = 0.2 μm) in H_2O by using negative-stained TEM at room temperature. DLS size distributions of 1 (b, 0.040 mM), 2 (d, 0.040 mM), and 3 (f, 0.040 mM) in DMSO/H_2O (v/v = 1:9), as well as 4 (h, 0.040 mM) in H_2O.

between the aromatic protons on pillararenes and the bipyridinium protons $H_{a,b}$ on **12** (Figure S8 in the SI). The inclusion complexes and their 1:1 host–guest stoichiometry were confirmed by high-resolution mass spectrometry (Figures S9–S12 in the SI). The complex constants (K) were calculated according to Benesi–Hildebrand equation[15–18] determined by UV–vis (Figure S13 in the SI) and fluorescence titrations (Figure S14 in the SI). The obtained K values are around $2–5 \times 10^3$ M^{-1} (Table S5 in the SI), in accordance with those average constants ($\sim 10^3$ M^{-1}) for 1:1 pillararene/viologen complexes reported in literature.[18]

MTT Assay and Confocal Laser Scattering Microscopy. In order to select a suitable pillararene complex for performing the bioimaging investigations, the cytotoxicity of the complexes and the effect on micromorphologies after adding **12** into the solutions of amphiphilic pillararenes were determined. As shown from the MTT assay (Figure S15 in the SI), the toxicity of **12** was tolerant for cells at low concentrations. In addition, the presence of biocompatible pillararenes **1** and **4** lowered the toxicity of **12**, while the compounds **2** and **3** made its toxicity even worse. Indeed, the complex of **3** and **12** is highly toxic to HeLa cells with the lowest cell viability under the same concentration measured. As shown from the TEM images, individual **12** cannot self-assemble into regular aggregates in H_2O (0.1 mM, Figure S16 in the SI), and the addition of **12** to the solutions containing **1**, **3**, and **4** did not affect their vesicular morphologies (Figure S17 in the SI). Furthermore, fluorescent assemblies were observed by fluorescent microscopy (Figure S17 in the SI), emitting significant fluorescence when

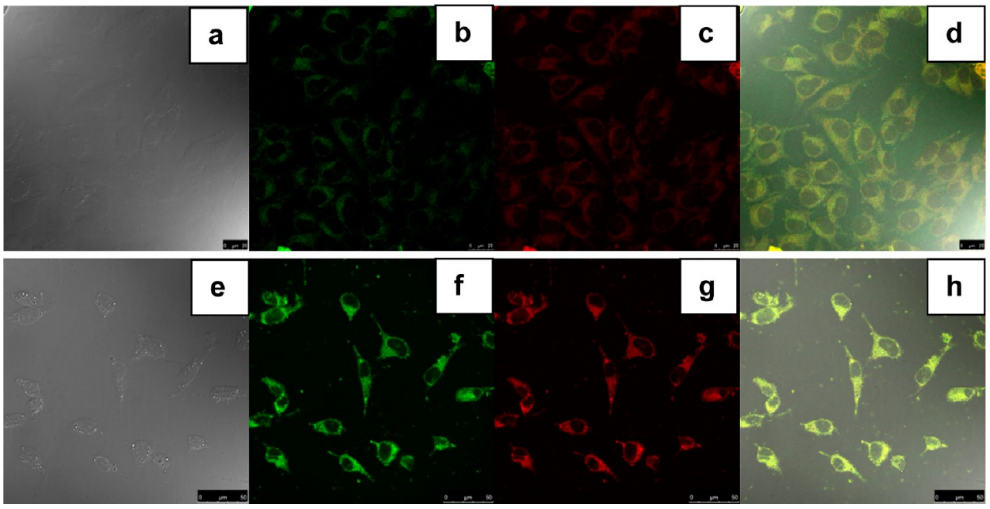

Figure 3. CLSM images of HeLa cells, after being treated with 1 (40 μM) containing FITC (4 μM) and RhB (4 μM) for 24 h: (a) bright field, (b) FITC channel, (c) RhB channel, and (d) merged image of (a−c), scale bar is 25 μm; and after being treated with 2 (40 μM) containing FITC (4 μM) and RhB (4 μM) for 24 h: (e) bright field, (f) FITC channel, (g) RhB channel, and (h) merged image of (e−g), scale bar is 50 μm.

excited at 488 nm. Based on the microscopy studies, it can be concluded that some pillararene/viologen complexes also have the capacity to undergo self-assembly (Scheme 1B). However, the complex formation between **2** and **12** led to the disappearance of both opalescent transparency in solution and assemblies determined under microscopy. DLS measurements in a variable concentration scale confirmed the sizes (50−300 nm) of the self-assemblies formed by the pillararene complexes of **1•12**, **3•12**, and **4•12** (Figures S18−S21 and Tables S6−S9 in the SI). Interestingly, the CAC of the complex **1•12** can only be determined by DLS. The presence of **12** enables bola-like amphiphiles **3** and **4** to form regular and stable assemblies much easier even at low concentrations and thus cannot provide exact CAC values for the complexes. The observation was further confirmed by UV−vis and fluorescent measurements under a variable concentration scale (Figures S22 and S23 in the SI). Thus, the complexes **1•12**, **3•12**, and **4•12** can be used for bioimaging applications owing to their relatively low cytotoxicity and the formations of stable self-assemblies.

To carry out the bioimaging investigations using these pillararene complexes, confocal laser scanning microscopy (CLSM) was employed.[30−32,39,40] As expected, HeLa cells could be imaged by compound **12** delivered by amphiphilic pillararene-based assemblies (**1**, **3**, and **4**), showing green intracellular color (Figure S24 in the SI). Complex **2•12** did not present bioimaging character as others since the complex cannot form the assembly and thus cannot serve as a carrier.

Delivery of Hydrophobic Dye by Pillararene-Based Assemblies. As a hydrophobic dye, FITC has a poor solubility in H_2O (less than 0.1 mg mL^{-1}) and is commonly used in biomodification and biolabeling with low cytotoxicity (Figure S25 in the SI).[27−29] FITC was chosen as another model dye to be delivered by pillararene-based assemblies. The cytotoxicity of amphiphilic pillararene-based assemblies (**1**−**4**) with FITC was determined by the MTT assay (Figure S25 in the SI). The obtained results indicate that all amphiphilic pillararene assemblies could increase the cytotoxicity of FITC above the concentration of 50 μM. The toxicity of pillararene-based assemblies (**1**, **3**, and **4**) containing FITC was acceptable with high cell viabilities below the concentration of 50 μM. In the case of assembly **2** with FITC, it showed very high cytotoxicity even below the concentration of 10 μM. Thus, further experiments were performed using the samples at suitable concentrations with good biocompatibility. In addition, FITC itself cannot form regular aggregates under the same conditions (Figure S16b in the SI), and adding FITC into the solutions of pillararenes **1**−**3** did not destroy the formed pillararene assemblies as confirmed by TEM (Figure S26 in the SI) and DLS (Figure S27 and Table S10 in the SI). Fluorescent objects can be observed in these sample solutions by fluorescent microscopy (Figure S26 in the SI). After adding FITC into the solution of the compound **4**, no regular assemblies can be observed by either TEM or fluorescent microscopy. Since FITC is a hydrophobic dye and cannot be included by the cavity of pillararenes, it can be easily included by hydrophobic layers of vesicular structures formed by tadpole-like amphiphilic pillararenes **1** and **2** with fluorescent emission (Scheme 1B).[15−18,36−38] Having methyl end groups on the structure of **3**, the formed lamellar spheres by **3** can also deliver FITC. On the other hand, the presence of hydrophobic FITC could destroy the membranes formed by bola-like amphiphilic pillararene **4**. Thus, pillararenes **1**−**3** performed better than **4** in terms of the FITC delivery. Since the

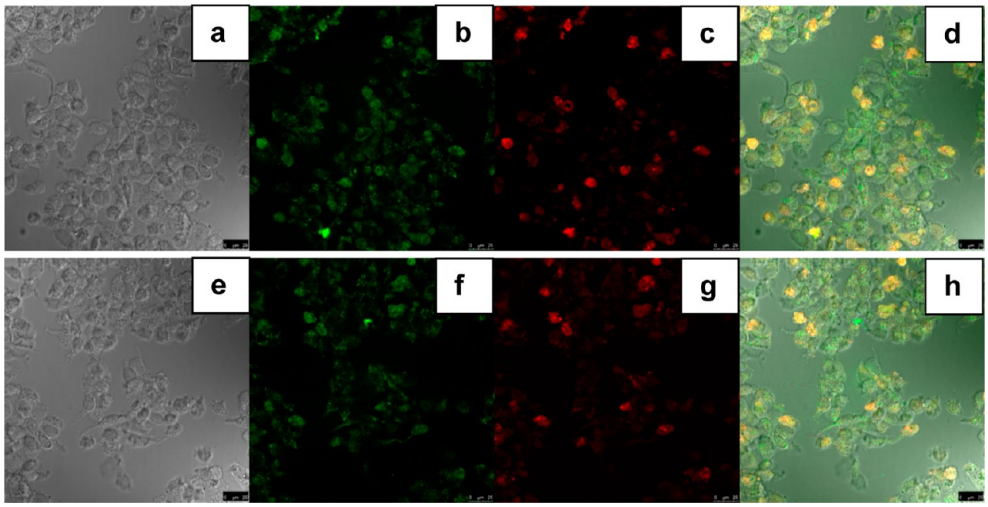

Figure 4. CLSM images of HeLa cells, after being treated with 1 (40 μM) containing 12 (40 μM) and RhB (4 μM) for 24 h: (a) bright field, (b) green field (exited at 488 nm), (c) RhB channel, and (d) merged image of (a−c), scale bar is 25 μm; after being treated with 4 (40 μM) containing 12 (40 μM) and RhB (4 μM) for 24 h: (e) bright field, (f) green field (exited at 488 nm), (g) RhB channel, and (h) merged image of (e−g), scale bar is 25 μm.

pillararene-based assemblies (**1**−**3**) containing FITC are biocompatible under suitable concentrations and have regular morphologies, we used them to carry out bioimaging application. As shown by CLSM images (Figure S28 in the SI), HeLa cells were stained green by FITC delivered from pillararene-based assemblies (**1**−**3**).

Delivery of Hydrophilic Dye by Pillararene-Based Assemblies. In contrast to hydrophobic FITC, RhB with high aqueous solubility (50 mg mL^{-1}) was chosen as the third model dye.[20−22] As determined by the MTT assay (Figure S29 in the SI), all pillararenes discussed here did not obviously increase the cytotoxicity of RhB below the concentration of 50 μM. From TEM investigations (Figure S16c in the SI), individual RhB cannot form regular assemblies in H_2O. The presence of RhB did not influence the morphologies formed by amphiphilic pillararenes **1**−**4** as confirmed by TEM, fluorescent microscopy (Figure S30 in the SI), and DLS (Figure S31 and Table S11 in the SI), and it emits fluorescence when excited at 515 nm. It was proposed that water-soluble RhB with large molecular size than the cavity of pillararenes was encapsulated into the aqueous cores inside vesicular structures (Scheme 1B).[36−38] Thus, biocompatible amphiphilic pillararenes **1**−**4** containing RhB were also used for bioimaging. As detected by CLSM (Figure S32 in the SI), RhB delivered by pillararene-based assemblies performed well in imaging HeLa cells in red.

Delivery of Mixed Dyes by Pillararene-Based Assemblies for Dual Bioimaging. These biocompatible amphiphilic pillararene-based assemblies possessing both pillararene cavities and assembled vesicular structures were confirmed to successfully deliver suitable guests, hydrophobic dye, and water-soluble dye for bioimaging. On the basis of these research results, we moved on by using these assemblies for the delivery of mixed dyes. Two groups of mixed dyes were employed here: group one contains FITC and RhB, while group two contains **12** and RhB. In the presence of group one, FITC and RhB, the assemblies formed by bola-like amphiphiles **3** and **4** were destroyed, but those assembled by tadpole-like amphiphiles **1** and **2** still existed without any significant changes as indicated by TEM observations and DLS measurements (Figures S33 and S34 and Table S12 in the SI). These two assemblies exhibited green (from FITC) and red (from RhB) colors when exited at 488 and 515 nm, respectively, observed by fluorescent microscopy (Figure S33 in the SI). It can be proposed that tadpole-like amphiphile-based vesicular assemblies containing bilayer structures and aqueous cores could include both hydrophobic and water-soluble dyes simultaneously (Scheme 1B).[36−38] CLSM observations further confirmed that tadpole-like amphiphile-based assemblies present remarkable performance on delivering both FITC and RhB to HeLa cells for imaging, showing green and red colors, respectively (Figure 3 and Figure S35 in the SI).

We then examined the group two, **12** and RhB, as mixed dyes for loading into pillararene-based assemblies. In comparison with destroyed morphologies of assemblies **2** and **3**, regular vesicular assemblies formed by compounds **1** and **4** in the presence of group two could still be observed, exhibiting fluorescent dots with various colors as confirmed by TEM, fluorescent microscopy, and DLS (Figures S33 and S34 and Table S12 in the SI). It is reasonable that the complexes between pillararenes (**1** and **4**) and **12** form assemblies in aqueous solution (Figure S17 in the SI), and thus assemblies obtained further wrap RhB within the aqueous cores (Scheme 1B). As expected, the assemblies based on pillararenes **1** and **4** can deliver simultaneously **12** and RhB to HeLa cells with green and red colors, as observed by CLSM (Figure 4 and Figure S36 in the SI).

Thus, amphiphilic pillararene-based assemblies have the capacity to deliver mixed dyes with different aqueous solubility and properties for dual bioimaging *in vitro*.

Delivery of Anticancer Drug by Pillararene-Based Assemblies. Furthermore, a real anticancer drug, Dox,[30−32] which can be dissolved in H_2O with the maximum concentration of 10 mg mL^{-1}, was delivered by these amphiphilic pillararene-based assemblies. As demonstrated by the MTT assay (Figure S37 in the SI), Dox-loaded pillararene assemblies showed decreasing cell viability at relatively high concentration above 50 μM, indicating that more Dox was delivered into cells by pillararene assemblies.[30−32] In comparison with individual Dox, the cytotoxicity of Dox-loaded pillararene assemblies was not increased a lot, suggesting that the encapsulation by pillararene-based assemblies delays the release of Dox *in vitro*. CLSM was then employed to monitor the delivery of Dox by the pillararene assemblies. As shown in Figure S38 of the SI, the pillararene assemblies carried Dox into cells and stained the cells clearly with red color, not only in cytoplasm but also in nucleus, proving that Dox was released into the nuclei.[30−32]

CONCLUSIONS

In conclusion, the current research has provided a successful example of using biocompatible pillararene-based assemblies to deliver mixed dyes for dual bioimaging *in vitro*. Interestingly, different types of amphiphilic pillararenes have exhibited different performance on the delivery of hydrophobic and hydrophilic dyes. All pillararene-based assemblies can deliver water-soluble RhB to cells, while only tadpole-like amphiphilic pillararene assemblies perform well on delivering hydrophobic FITC for bioimaging. Pillararenes **1**, **3**, and **4** could complex with fluorescent electron acceptor guest **12** to further form stable assemblies for bioimaging. During the investigations of delivering mixed dyes for dual bioimaging, tadpole-like amphiphilic assembly **1** presents the best performance. Finally, anticancer drug, Dox, has been successfully delivered into cells by pillararene-based assemblies. The current research has demonstrated the capacities of pillararene-based assemblies on delivering different types of dyes *in vitro* and has paved the way for employing these biocompatible carriers to deliver mixed drugs toward combined and enhanced cancer therapy.

MATERIALS AND METHODS

Characterization. ^{1}H nuclear magnetic resonance (^{1}H NMR) spectra were recorded at room temperature on Bruker Avance 300/400 with working frequencies of 300/400 MHz for ^{1}H and 75 MHz for ^{13}C nuclei. All ^{13}C NMR spectra were recorded with the simultaneous decoupling of ^{1}H nuclei. The following abbreviations were used to explain the multiplicities: s, singlet; d, doublet; t, triplet; b, broad peaks; m, multiplet or overlapping peaks. The high-resolution time-of-flight mass spectrometry (TOF MS) was performed on a Waters Q-tof Premier MS spectrometer. Elemental analysis was performed on a EuroVector Euro EA elemental analyzer.

Procedures for Synthesis of DMpillar,[5,6] DBpillar,[5,6] and Compounds 5−7[41,42]. Corresponding monomer as the starting material reacted with an equivalent amount of paraformaldehyde and boron trifluoride diethyl etherate in refluxing 1,2-dichloroethane under a nitrogen atmosphere (Scheme S1). The crude product obtained was directly subjected to column chromatography (SiO_2, gradient elution from 40 to 90% CH_2Cl_2 in *n*-hexane) to afford target product.

DMpillar:. 19% yield, white powder. ^{1}H NMR (300 MHz, $CDCl_3$): δ = 6.76 (s, 10.0H), 3.77 (s, 9.7H), 3.64 (s, 28.6H). ESI-MS: 751.23 $[M + H]^+$.

DBpillar:. 20% yield, white powder. The DBpillar was synthesized by using compound **S2** (Scheme S1) as the starting material according to the reported method.[1−3] ^{1}H NMR (300 MHz, Me_2CO-d_6): δ = 6.91 (s, 10.0H), 3.88 (t, 19.0H), 3.74 (s, 9.47H), 1.89−1.79 (m, 19.4H), 1.64−1.56 (m, 19.7H), 1.03 (t, J = 6 Hz, 28.7H). ^{13}C NMR (75 MHz, Me_2CO-d_6): δ = 149.6, 128.3, 114.3, 67.8, 31.9, 19.3, 13.5. HR-MS (ESI): $C_{75}H_{111}O_{10}$ calcd for m/z = 1171.8177, found m/z = 1171.8027 $[M + H]^+$.

Compound 5:. 8.6% average yield, white powder. ^{1}H NMR (300 MHz, Me_2CO-d_6): δ = 6.96 (t, J = 3 Hz, 5.0H), 6.87 (d, J = 9 Hz, 4.9), 4.66 (t, J = 3 Hz, 10.6H), 3.77−3.75 (m, 26.5H), 2.97−2.94 (m, 5.0H). ^{13}C NMR (75 MHz, Me_2CO-d_6): δ = 150.9, 148.6, 128.3, 114.7, 113.3, 79.6, 75.5, 56.1, 55.0, 54.0, 40.5. HR-MS (ESI): $C_{55}H_{51}O_{10}$ calcd for m/z = 871.3482, found m/z = 871.3514 $[M + H]^+$.

Compound 6:. 8.8% average yield, white powder. ^{1}H NMR (300 MHz, Me_2CO-d_6): δ = 6.96 (s, 4.4H), 6.87 (s, 4.3H) 4.68 (t, 10.1H), 3.98−3.88 (m, 11.2H), 3.76 (d, J = 9 Hz, 10.0H), 2.99−2.94 (m, 4.4H), 1.84 (s, 11.3H), 1.62 (t, J = 6 Hz, 11.3H), 1.03 (t, J = 6 Hz, 15.0H). ^{13}C NMR (75 MHz, Me_2CO-d_6): δ = 150.3, 148.5, 128.6, 128.1, 114.4, 114.3, 80.2, 75.1, 67.8, 56.1, 55.9, 31.9, 19.4, 13.5. HR-MS (ESI): $C_{70}H_{81}O_{10}$ calcd for m/z = 1081.5830, found m/z = 1081.5966 $[M + H]^+$.

Compound 7:. 12% yield, white powder. ^{1}H NMR (300 MHz, Me_2CO-d_6): δ = 7.01 (s, 10.0H), 4.71 (s, 19.8H), 3.78 (s, 10.0H), 3.01 (t, J = 3 Hz, 9.3H). ^{13}C NMR (75 MHz, Me_2CO-d_6): δ = 149.1, 128.4, 114.5, 79.4, 75.7, 56.1. HR-MS (ESI): $C_{65}H_{51}O_{10}$ calcd for m/z = 991.3482, found m/z = 991.3438 $[M + H]^+$.

Procedures for Synthesis of Compounds 1−4. Corresponding alkynyl pillararenes (**5**−**7**) as the starting materials were mixed with an equivalent amount of azido-modified ethylene glycol derivatives (**S7** and **S9**, Scheme S1), tris[(1-benzyl-1*H*-1,2,3-triazol-4-yl)-methyl]amine (TBTA), and tetrakis(acetonitrile) copper(I) hexafluorophosphate in refluxing Me_2CO under nitrogen atmosphere. The mixture solution was stirred under reflux for 2 days. The crude solution was then poured into H_2O. The aqueous phase was extracted (3 × 200 mL) with CH_2Cl_2. The combined organic layers were dried (Mg_2SO_4), and the solvent was removed in vacuum. The mixture was subjected to column chromatography (SiO_2, gradient elution from 5 to 10% MeOH in CH_2Cl_2) to afford target product.

Compound 1:. 80% yield, light yellow oil. ^{1}H NMR (300 MHz, Me_2CO-d_6): δ = 8.08 (d, J = 9 Hz, 5.0H), 7.09−6.86 (m, 11.5H), 5.14 (s, 5.8 H), 4.90 (d, J = 9 Hz, 4.4H), 4.57−4.50 (m, 10.9H), 3.82−3.21 (m, 94.1H). ^{13}C NMR (75 MHz, Me_2SO-d_6): δ = 162.8, 150.7, 149.0, 143.7, 127.8, 124.8, 114.9, 113.5, 72.8, 70.2, 69.1, 62.4, 60.7, 55.8, 50.5, 49.9, 36.2, 31.2, 29.2. HR-MS (ESI): $C_{95}H_{136}N_{15}O_{30}$ calcd for m/z = 1966.9578, found m/z = 1966.9583 $[M + H]^+$. Anal. Calcd for $C_{95}H_{135}N_{15}O_{30}$: C, 58.00; H, 6.92; N, 10.68. Found: C, 57.58; H, 7.02; N, 10.30.

Compound 2:. 81% yield, dark yellow oil. ^{1}H NMR (300 MHz, Me_2CO-d_6): δ = 8.11−8.06 (m, 4.6H), 7.10−6.84 (m, 10.0H), 5.13 (s, 4.7H), 4.87 (s, 4.1H), 4.58−4.50 (m, 8.0H), 3.90−3.38

(m, 92.8H), 1.85−1.77 (m, 11.2H), 1.61 (s, 11.6H), 1.07−0.98 (m, 17.2H). ^{13}C NMR (75 MHz, Me_2SO-d_6): δ = 162.6, 149.6, 148.8, 143.8, 128.7, 124.6, 114.8, 114.1, 72.8, 69.9, 67.7, 61.9, 60.6, 50.4, 49.8, 36.3, 31.7, 31.2, 28.9, 19.4, 14.3. HR-MS (ESI): $C_{110}H_{166}N_{15}O_{30}$ calcd for m/z = 2177.1925, found m/z = 2177.1885 $[M + H]^+$. Anal. Calcd for $C_{110}H_{165}N_{15}O_{30}$: C, 60.67; H, 7.64; N, 9.65. Found: C, 60.40; H, 7.72; N, 9.29.

Compound 3:. 85% yield, light yellow oil. ^{1}H NMR (300 MHz, Me_2CO-d_6): δ = 8.13 (s, 10.0H), 7.07 (s, 9.7H), 5.02 (s, 10.0H), 4.89 (s, 10.3H), 4.46 (s, 21.1H), 3.78 (s, 32.4H), 3.41−3.30 (m, 42.0H), 3.20 (s, 34.6H). ^{13}C NMR (75 MHz, Me_2SO-d_6): δ = 149.3, 128.3, 114.9, 78.9, 71.4, 69.7, 69.0, 61.6, 58.4, 49.9. HR-MS (ESI): $C_{115}H_{161}N_{30}O_{30}$ calcd for m/z = 2442.1995, found m/z = 2442.1917 $[M + H]^+$. Anal. Calcd for $C_{115}H_{160}N_{30}O_{30}$: C, 56.55; H, 6.60; N, 17.20. Found: C, 56.23; H, 6.69; N, 16.79.

Compound 4:. 81% yield, light yellow oil. ^{1}H NMR (300 MHz, Me_2CO-d_6): δ = 8.16 (s, 10.5H), 7.06 (s, 10.0H), 4.99 (d, J = 8 Hz, 8.2H), 4.85 (d, J = 8 Hz, 9.0H), 4.56 (s, 22.2H), 3.80 (s, 37.6H), 3.60−3.46 (m, 102.6H), 3.33−3.28 (m, 25.4H). ^{13}C NMR (75 MHz, D_2O): δ = 146.8, 141.9, 126.8, 122.8, 113.3, 69.5, 67.3, 66.7, 59.1, 58.1, 47.8. HR-MS (ESI): $C_{145}H_{221}N_{30}O_{50}$ calcd for m/z = 3182.5673, found m/z = 3182.5679 $[M + H]^+$. Anal. Calcd for $C_{145}H_{220}N_{30}O_{50}$: C, 54.71; H, 6.97; N, 13.20. Found: C, 54.35; H, 7.06; N, 12.73.

Procedures for Synthesis of Compounds 8−11. Corresponding alkynyl benzene derivatives (**S3**−**S5**, Scheme S1) as the starting materials were mixed with equivalent amount of azido-modified ethylene glycol derivatives (**S7** and **S9**, Scheme S1), tris[(1-benzyl-1*H*-1,2,3-triazol-4-yl)methyl]amine (TBTA), and tetrakis(acetonitrile) copper(I) hexafluorophosphate in refluxing Me_2CO under nitrogen atmosphere. The obtained crude product was subjected to column chromatography (SiO_2, gradient elution from 2 to 9% MeOH in CH_2Cl_2) to afford target product.

Compound 8:. 86% yield, yellow oil. ^{1}H NMR (400 MHz, Me_2SO-d_6): δ = 8.17 (s, 1.0H), 6.98 (t, J = 4 Hz, 2.0H), 6.87 (t, J = 4 Hz, 2.0H), 5.08 (s, 2.0H), 4.59−4.53 (m, 2.9H), 3.83 (t, J = 4 Hz, 2.0H), 3.71 (s, 3.1H), 3.55−3.47 (m, 10.9H), 3.41 (t, J = 4 Hz, 2.0H). ^{13}C NMR (75 MHz, Me_2SO-d_6): δ = 154.0, 152.4, 143.4, 125.2, 116.1, 115.0, 72.8, 70.0, 69.1, 62.0, 60.7, 55.8, 49.9. HR-MS (ESI): $C_{18}H_{28}N_3O_6$ calcd for m/z = 382.1978, found m/z = 382.2007 $[M + H]^+$. Anal. Calcd for $C_{18}H_{27}N_3O_6$: C, 56.68; H, 7.13; N, 11.02. Found: C, 56.42; H, 7.19; N, 10.82.

Compound 9:. 87% yield, yellow oil. ^{1}H NMR (400 MHz, Me_2SO-d_6): δ = 8.17 (s, 1.0H), 6.95 (t, J = 4 Hz, 2.0H), 6.86 (t, J = 4 Hz, 2.3H), 5.07 (s, 2.0H), 4.59−4.53 (m, 3.0H), 3.90 (t, J = 4 Hz, 2.3H), 3.83 (s, 2.0H), 3.54−3.47 (m, 10.7H), 3.41 (t, J = 4 Hz, 2.1H), 1.69−1.64 (m, 2.3H), 1.46−1.41 (m, 2.3H), 0.94 (t, J = 4 Hz, 3.5H). ^{13}C NMR (75 MHz, Me_2SO-d_6): δ = 153.5, 152.5, 143.3, 125.2, 116.1, 115.7, 72.8, 70.1, 69.2, 68.0, 62.1, 60.7, 49.9, 31.3, 19.2, 14.2. HR-MS (ESI): $C_{21}H_{34}N_3O_6$ calcd for m/z = 424.2448, found m/z = 424.2423 $[M + H]^+$. Anal. Calcd for $C_{21}H_{33}N_3O_6$: C, 59.56; H, 7.85; N, 9.92. Found: C, 59.42; H, 7.89; N, 9.69.

Compound 10:. 84% yield, light yellow powder. ^{1}H NMR (300 MHz, Me_2CO-d_6): δ = 8.04 (s, 2.0H), 6.97 (s, 4.2H), 5.11 (s, 4.1H), 4.57 (t, J = 6 Hz, 4.1H), 3.89 (t, J = 3 Hz, 4.2H), 3.58 (t, J = 6 Hz, 4.1H), 3.45 (t, J = 6 Hz, 4.1H), 3.26 (s, 6.0H). ^{13}C NMR (75 MHz, Me_2CO-d_6): δ = 153.0, 115.7, 71.6, 70.0, 69.2, 62.1, 57.9, 49.9. HR-MS (ESI): $C_{22}H_{33}N_6O_6$ calcd for m/z = 477.2462, found m/z = 477.2477 $[M + H]^+$. Anal. Calcd for $C_{22}H_{32}N_6O_6$: C, 55.45; H, 6.77; N, 17.64. Found: C, 55.32; H, 6.81; N, 17.40.

Compound 11:. 82% yield, yellow oil. ^{1}H NMR (300 MHz, D_2O): δ = 7.97 (s, 2.0H), 6.86 (s, 3.9H), 5.04 (s, 3.9H), 4.49 (t, J = 3 Hz, 4.3H), 3.82 (t, J = 6 Hz, 4.3H), 3.62−3.54 (m, 8.0H), 3.45 (d, J = 9 Hz, 18.0H). ^{13}C NMR (75 MHz, D_2O): δ = 164.9, 152.1, 143.3, 125.5, 116.3, 71.7, 69.5, 68.7, 61.7, 60.3, 50.0, 36.9, 31.4. HR-MS (ESI): $C_{28}H_{45}N_6O_{10}$ calcd for m/z = 625.3197, found m/z = 625.3193 $[M + H]^+$. Anal. Calcd for $C_{28}H_{44}N_6O_{10}$: C, 53.84; H, 7.10; N, 13.45. Found: C, 53.59; H, 7.17; N, 13.08.

Procedures for Synthesis of DHpillar and Compound 12. DHpillar was synthesized by using DMpillar as the starting material according to the reported method.[5] ^{1}H NMR (400 MHz, Me_2CO-d_6): δ = 6.67 (s, 10.0H), 3.59 (s, 10.7H). ESI-MS: 610.84 [M].

Compound **12** was synthesized by using 4,4′-dipyridyl and 1-bromobutane as the starting materials according to the previous reports:[10,43] 91% yield, yellow powder. ^{1}H NMR (300 MHz, D_2O): δ = 9.05 (d, J = 6 Hz, 4.0H), 8.48 (s, 3.9H), 2.16 (s, 2.5H), 2.00 (s, 4.1H), 1.34 (d, J = 6 Hz, 4.1H), 0.91 (d, J = 6 Hz, 5.9H). ^{13}C NMR (75 MHz, D_2O): δ = 147.3, 142.7, 124.2, 59.3, 29.9, 16.0, 9.9. HR-MS (ESI): $C_{18}H_{26}N_2Br$ calcd for m/z = 349.1279, found m/z = 349.1250 $[M]^+$.

Preparation and Characterization of Sample Solutions. The stock solutions (1×10^{-1} mol L^{-1} and 1×10^{-3} mol L^{-1}) of pillararenes and their complexes were prepared with HPLC-grade DMSO and deionized (DI) water. DI water was triply distilled. All the sample solutions for detecting complex constants (K) and variable concentration investigations were freshly prepared by diluting the stock solutions according to literature procedures.[11] UV−vis spectra were recorded with Shimadzu UV-3600 UV−vis−NIR spectrophotometer at 298 K. The emission spectra were recorded on a Varian Cary Eclipse fluorescence spectrophotometer.

Characterization of Morphology and Sizes. Negative-stained TEM images was recorded on a JEM 1400 electron microscope (120 kV) equipped with slow scan CCD and using cold cathode field emission as the gun. The samples for negative-stained TEM were prepared by dropping a droplet of the orange sample solution onto a TEM grid (copper grid, 300 meshes, coated with carbon film), immediately followed by staining with 1% sodium phosphotungstate in H_2O (about 2 μL) and allowing to air-dry. The fluorescence microscopic images were taken by a confocal fluorescence microscope (Nikon, Eclipse TE2000-E, 60× oil objective). DLS measurements were carried out with a Zetasizer Nano ZS instrument from Malvern Instruments Ltd. at 298 K using a 633 nm "red" laser. The mean hydrodynamic size was calculated with Zetasizer software.

Cell Culture. HeLa (human cervical cancer) cells were cultured in DMEM medium containing 10% fetal bovine serum (FBS) and 2% antibiotics in a humidified atmosphere with 5% CO_2 at 37 °C.[30−32,39]

MTT Cytotoxicity Assay. The cytotoxicity of pillararenes and their complexes with dyes was evaluated by employing the MTT assay.[30−32,39] HeLa cells were seeded into a 96-well plate at a density of 1×10^4 cells/well in DMEM medium. After 24 h exposure, the medium in the wells was replaced with fresh medium (100 μL) containing determination substrates, that is, pillararenes and their complexes with dyes, with gradually diluted concentrations according to standard procedure.[30,31] After incubation for another 24 h, the medium was removed and medium (100 μL) containing MTT (0.5 mg mL^{-1}) was added. After further incubation for 4 h, the medium was replaced with DMSO (100 μL). The plate was gently shaked for 30 min. Then, the absorbance at 560 nm was recorded using a microplate reader (infinite 200 PRO, Tecan). The cell viability related to the control wells that only contain cell culture medium was calculated by $[A]_{test}/[A]_{control}$, where $[A]_{test}$ and $[A]_{control}$ are the average absorption intensities of the test and control samples, respectively.

Fluorescence Microscopic Images. HeLa cells were seeded in plastic bottomed μ-dishes (35 mm) and grown in the DMEM medium for 24 h. After HeLa cells were exposed to the detecting substrates (pillararenes and their complexes with dyes) for 24 h, the medium was removed and dishes were washed three times with phosphate buffered saline (PBS) buffer and fixed with 4.0% paraformaldehyde at room temperature for 15 min. After washing with PBS, the cells were observed and taken images by a confocal fluorescence microscope (Nikon, Eclipse TE2000-E, 60× oil objective).

Conflict of Interest: The authors declare no competing financial interest.

Acknowledgment. This work was financially supported by the Singapore National Research Foundation Fellowship (NRF2009NRF-RF001-015), the Singapore National Research Foundation CREATE program−Singapore Peking University Research Centre for a Sustainable Low-Carbon Future, and the Centre of Excellence for Silicon Technologies (A*Star SERC No.: 112 351 0003). Authors would like to thank Dr. Yongfei Zeng for technical assistance on elemental analysis, and Dr. Zhong Luo for helpful discussions on cytotoxicity and cell studies.

Supporting Information Available: Synthesis and characterization, MTT assay, DLS data of different assemblies under

various concentrations, TEM images of different assemblies, ^{1}H NOESY NMR spectra, TOF mass spectra, UV spectra, fluorescent emission spectra, fluorescent microscopy images of different assemblies, confocal laser scanning microscopic images of HeLa cells with different assemblies, and characterization spectra of compounds. This material is available free of charge *via* the Internet at http://pubs.acs.org.

REFERENCES AND NOTES

1. Ogoshi, T. Synthesis of Novel Pillar-Shaped Cavitands "Pillar[5]arenes" and Their Application for Supramolecular Materials. *J. Inclusion Phenom. Macrocyclic Chem.* **2012**, *72*, 247–262.
2. Cragg, P. J.; Sharma, K. Pillar[5]arenes: Fascinating Cyclophanes with a Bright Future. *Chem. Soc. Rev.* **2012**, *41*, 597–607.
3. Xue, M.; Yang, Y.; Chi, X.; Zhang, Z.; Huang, F. Pillararenes, A New Class of Macrocycles for Supramolecular Chemistry. *Acc. Chem. Res.* **2012**, *45*, 1294–1308.
4. Meier, H.; Cao, D. Neue Gastfreundliche Wirtmoleküle. *Nachr. Chem.* **2013**, *61*, 408–410.
5. Ogoshi, T.; Kanai, S.; Fujinami, S.; Yamagishi, T.; Nakamoto, Y. *para*-Bridged Symmetrical Pillar[5]arenes: Their Lewis Acid Catalyzed Synthesis and Host–Guest Property. *J. Am. Chem. Soc.* **2008**, *130*, 5022–5023.
6. Cao, D.; Kou, Y.; Liang, J.; Chen, Z.; Wang, L.; Meier, H. A Facile and Efficient Preparation of Pillararenes and a Pillarquinone. *Angew. Chem., Int. Ed.* **2009**, *48*, 9721–9723.
7. Zhang, Z.; Luo, Y.; Chen, J.; Dong, S.; Yu, Y.; Ma, Z.; Huang, F. Formation of Linear Supramolecular Polymers That Is Driven by CH···π Interactions in Solution and in the Solid State. *Angew. Chem., Int. Ed.* **2011**, *50*, 1397–1401.
8. Si, W.; Chen, L.; Hu, X. B.; Tang, G.; Chen, Z.; Hou, J. L.; Li, Z. T. Selective Artificial Transmembrane Channels for Protons by Formation of Water Wires. *Angew. Chem., Int. Ed.* **2011**, *50*, 12564–12568.
9. Strutt, N. L.; Fairen-Jimenez, D.; Iehl, J.; LaLonde, M. B.; Snurr, R. Q.; Farha, O. K.; Hupp, J. T.; Stoddart, J. F. Incorporation of An A1/A2-Difunctionalized Pillar[5]arene into a Metal–Organic Framework. *J. Am. Chem. Soc.* **2012**, *134*, 17436–17439.
10. Yao, Y.; Xue, M.; Chen, J.; Zhang, M.; Huang, F. An Amphiphilic Pillar[5]arene: Synthesis, Controllable Self-Assembly in Water, and Application in Calcein Release and TNT Adsorption. *J. Am. Chem. Soc.* **2012**, *134*, 15712–15715.
11. Yu, G.; Xue, M.; Zhang, Z.; Li, J.; Han, C.; Huang, F. A Water-Soluble Pillar[6]arene: Synthesis, Host–Guest Chemistry, and Its Application in Dispersion of Multiwalled Carbon Nanotubes in Water. *J. Am. Chem. Soc.* **2012**, *134*, 13248–13251.
12. Chen, Y.; Cao, D.; Wang, L.; He, M.; Zhou, L.; Schollmeyer, D.; Meier, H. Monoester Copillar[5]arenes: Synthesis, Unusual Self-Inclusion Behavior, and Molecular Recognition. *Chem.—Eur. J.* **2013**, *19*, 7064–7070.
13. Li, H.; Chen, D. X.; Sun, Y. L.; Zheng, Y. B.; Tan, L. L.; Weiss, P. S.; Yang, Y. W. Viologen-Mediated Assembly of and Sensing with Carboxylatopillar[5]arene-Modified Au Nanoparticles. *J. Am. Chem. Soc.* **2013**, *135*, 1570–1576.
14. Gao, L.; Zheng, B.; Yao, Y.; Huang, F. Responsive Reverse Giant Vesicles and Gel from Self-Organization of a Bolaamphiphilic Pillar[5]arene. *Soft Matter* **2013**, *9*, 7314–7319.
15. Zhang, H.; Strutt, N. L.; Stoll, R. S.; Li, H.; Zhu, Z.; Stoddart, J. F. Dynamic Clicked Surfaces Based on Functionalised Pillar[5]arene. *Chem. Commun.* **2011**, *47*, 11420–11422.
16. Zhang, H.; Ma, X.; Guo, J.; Nguyen, K. T.; Zhang, Q.; Wang, X. J.; Yan, H.; Zhu, L.; Zhao, Y. Thermo-Responsive Fluorescent Vesicles Assembled by Fluorescein-Functionalized Pillar[5]arene. *RSC Adv.* **2013**, *3*, 368–371.
17. Zhang, H.; Nguyen, K. T.; Ma, X.; Yan, H.; Guo, J.; Zhu, L.; Zhao, Y. Host–Guest Complexation Driven Dynamic Supramolecular Self-Assembly. *Org. Biomol. Chem.* **2013**, *11*, 2070–2074.
18. Strutt, N.; Zhang, H.; Giesener, M. A.; Lei, J.; Stoddart, J. F. A Self-Complexing and Self-Assembling Pillar[5]arene. *Chem. Commun.* **2012**, *48*, 1647–1649.
19. Stoddart, J. F. From Supramolecular to Systems Chemistry: Complexity Emerging out of Simplicity. *Angew. Chem., Int. Ed.* **2012**, *51*, 12902–12903.
20. Liu, Z.; Qiao, J.; Niu, Z.; Wang, Q. Natural Supramolecular Building Blocks: From Virus Coat Proteins to Viral Nanoparticles. *Chem. Soc. Rev.* **2012**, *41*, 6178–6194.
21. Yang, K.; Feng, L.; Shi, X.; Liu, Z. Nano-Graphene in Biomedicine: Theranostic Applications. *Chem. Soc. Rev.* **2013**, *42*, 530–547.
22. Zhang, H.; Grüner, G.; Zhao, Y. Recent Advancements of Graphene in Biomedicine. *J. Mater. Chem. B* **2013**, *1*, 2542–2567.
23. Chen, Y.; Liu, Y. Cyclodextrin-Based Bioactive Supramolecular Assemblies. *Chem. Soc. Rev.* **2010**, *39*, 495–505.
24. Nimse, S. B.; Kim, T. Biological Applications of Functionalized Calixarenes. *Chem. Soc. Rev.* **2013**, *42*, 366–386.
25. Yu, G.; Zhou, X.; Zhang, Z.; Han, C.; Mao, Z.; Gao, C.; Huang, F. Pillar[6]arene/Paraquat Molecular Recognition in Water: High Binding Strength, pH-Responsiveness, and Application in Controllable Self-Assembly, Controlled Release, and Treatment of Paraquat Poisoning. *J. Am. Chem. Soc.* **2012**, *134*, 19489–19497.
26. Yu, G.; Ma, Y.; Han, C.; Yao, Y.; Tang, G.; Mao, Z.; Gao, C.; Huang, F. A Sugar-Functionalized Amphiphilic Pillar[5]arene: Synthesis, Self-Assembly in Water, and Application in Bacterial Cell Agglutination. *J. Am. Chem. Soc.* **2013**, *135*, 10310–10313.
27. Kim, S. T.; Saha, K.; Kim, C.; Rotello, V. M. The Role of Surface Functionality in Determining Nanoparticle Cytotoxicity. *Acc. Chem. Res.* **2013**, *46*, 681–691.
28. Sapsford, K. E.; Algar, W. R.; Berti, L.; Gemmill, K. B.; Casey, B. J.; Oh, E.; Stewart, M. H.; Medintz, I. L. Functionalizing Nanoparticles with Biological Molecules: Developing Chemistries That Facilitate Nanotechnology. *Chem. Rev.* **2013**, *113*, 1904–2074.
29. Lu, X.; Liu, Y.; Kong, X.; Lobie, P. E.; Chen, C.; Zhu, T. Nanotoxicity: A Growing Need for Study in the Endocrine System. *Small* **2013**, *9*, 1654–1671.
30. Ma, X.; Nguyen, K. T.; Borah, P.; Ang, C. Y.; Zhao, Y. Functional Silica Nanoparticles for Redox-Triggered Drug/ssDNA Co-delivery. *Adv. Healthcare Mater.* **2012**, *1*, 690–697.
31. Zhang, Q.; Liu, F.; Nguyen, K. T.; Ma, X.; Wang, X.; Xing, B.; Zhao, Y. Multifunctional Mesoporous Silica Nanoparticles for Cancer-Targeted and Controlled Drug Delivery. *Adv. Funct. Mater.* **2012**, *22*, 5144–5156.
32. Sreejith, S.; Ma, X.; Zhao, Y. Graphene Oxide Wrapping on Squaraine-Loaded Mesoporous Silica Nanoparticles for Bioimaging. *J. Am. Chem. Soc.* **2012**, *134*, 17346–17349.
33. Ma, X.; Ong, O. S.; Zhao, Y. Dual-Responsive Drug Release from Oligonucleotide-Capped Mesoporous Silica Nanoparticles. *Biomater. Sci.* **2013**, *1*, 912–917.
34. Kou, Y.; Tao, H.; Cao, D.; Fu, Z.; Schollmeyer, D.; Meier, H. Synthesis and Conformational Properties of Nonsymmetric Pillar[5]arenes and Their Acetonitrile Inclusion Compounds. *Eur. J. Org. Chem.* **2010**, *2010*, 6464–6470.
35. Zhang, Z.; Luo, Y.; Xia, B.; Han, C.; Yu, Y.; Chen, X.; Huang, F. Four Constitutional Isomers of BMpillar[5]arene: Synthesis, Crystal Structures and Complexation with *n*-Octyltrimethyl Ammonium Hexafluorophosphate. *Chem. Commun.* **2011**, *47*, 2417–2419.
36. Wang, Y.; Xu, H.; Zhang, X. Tuning the Amphiphilicity of Building Blocks: Controlled Self-Assembly and Disassembly for Functional Supramolecular Materials. *Adv. Mater.* **2009**, *21*, 2849–2864.
37. Chen, G.; Jiang, M. Cyclodextrin-Based Inclusion Complexation Bridging Supramolecular Chemistry and Macromolecular Self-Assembly. *Chem. Soc. Rev.* **2011**, *40*, 2254–2266.
38. Dong, R.; Liu, W.; Hao, J. Soft Vesicles in the Synthesis of Hard Materials. *Acc. Chem. Res.* **2012**, *45*, 504–513.

39. Yan, H.; Teh, C.; Sreejith, S.; Zhu, L.; Kwok, A.; Fang, W.; Ma, X.; Nguyen, K. T.; Korzh, V.; Zhao, Y. Functional Mesoporous Silica Nanoparticles for Photothermal-Controlled Drug Delivery *in Vivo*. *Angew. Chem., Int. Ed.* **2012**, *51*, 8373–8377.
40. Zhu, L.; Li, X.; Zhang, Q.; Ma, X.; Li, M.; Zhang, H.; Luo, Z.; Ågren, H.; Zhao, Y. Unimolecular Photoconversion of Multicolor Luminescence on Hierarchical Self-Assemblies. *J. Am. Chem. Soc.* **2013**, *135*, 5175–5182.
41. Yu, G.; Zhang, Z.; Han, C.; Xue, M.; Zhou, Q.; Huang, F. A Non-symmetric Pillar[5]arene-Based Selective Anion Receptor for Fluoride. *Chem. Commun.* **2012**, *48*, 2958–2960.
42. Ogoshi, T.; Shiga, R.; Hashizume, M.; Yamagishi, T. "Clickable" Pillar[5]arenes. *Chem. Commun.* **2011**, *47*, 6927–6929.
43. Li, C.; Xu, Q.; Li, J.; Yao, F.; Jia, X. Complex Interactions of Pillar[5]arene with Paraquats and Bis(pyridinium) Derivatives. *Org. Biomol. Chem.* **2010**, *8*, 1568–1576.